Sensitivity of OMI SO2 measurements to variable eruptive behaviour at Soufrière Hills Volcano, Montserrat

Journal of Volcanology and Geothermal Research 312 (2016) 1–10

Contents lists available at ScienceDirect

Journal of Volcanology and Geothermal Research

journal homepage: www.elsevier.com/locate/jvolgeores

Sensitivity of OMI SO_2 measurements to variable eruptive behaviour at Soufrière Hills Volcano, Montserrat

C.S. Hayer [a,*], G. Wadge [a], M. Edmonds [b], T. Christopher [c,d]

[a] ESSC, Dept. of Meteorology, University of Reading, Reading RG6 6AL, UK
[b] COMET+, Department of Earth Sciences, University of Cambridge, Cambridge CB2 3EQ, UK
[c] Montserrat Volcano Observatory, Montserrat
[d] Seismic Research Centre, University of West Indies, St. Augustine, Trinidad and Tobago

ARTICLE INFO

Article history:
Received 13 October 2015
Accepted 22 January 2016
Available online 29 January 2016

Keywords:
Volcanic plumes
Soufrière Hills Volcano
OMI
SO_2

ABSTRACT

Since 2004, the satellite-borne Ozone Mapping Instrument (OMI) has observed sulphur dioxide (SO_2) plumes during both quiescence and effusive eruptive activity at Soufrière Hills Volcano, Montserrat. On average, OMI detected a SO_2 plume 4–6 times more frequently during effusive periods than during quiescence in the 2008–2010 period. The increased ability of OMI to detect SO_2 during eruptive periods is mainly due to an increase in plume altitude rather than a higher SO_2 emission rate. Three styles of eruptive activity cause thermal lofting of gases (Vulcanian explosions; pyroclastic flows; a hot lava dome) and the resultant plume altitudes are estimated from observations and models. Most lofting plumes from Soufrière Hills are derived from hot domes and pyroclastic flows. Although Vulcanian explosions produced the largest plumes, some produced only negligible SO_2 signals detected by OMI. OMI is most valuable for monitoring purposes at this volcano during periods of lava dome growth and during explosive activity.

1. Introduction

Sulphur dioxide (SO_2) has a strong absorption signature in the UV and a low background abundance in the atmosphere, both of which facilitate its measurement in volcanic plumes and make SO_2 emission rate a valuable volcano monitoring tool (e.g. Edmonds et al., 2003a; Shinohara, 2008; Oppenheimer et al., 2011). Satellite observations of volcanic SO_2 emissions, although of lower resolution, complement ground-based spectrometer systems, which may not be effective during ash-producing eruptive events (Christopher et al., 2010) or for measuring vertically-rising plumes.

There have been many observations of volcanic SO_2 plumes from space-borne instruments. However, there have been few opportunities to compare these observations with ground-based instruments, and even fewer that allow for the assessment of their complementarity. Soufrière Hills volcano has a well-established ground-based instrument array along with other monitoring data (seismometers, GPS, tiltmeters, infrasound monitors). This provides an ideal test case to investigate the ground- and satellite-based measurement of SO_2 emission at a volcano with a highly variable, but well constrained, activity level.

In this paper, we conduct an analysis of OMI observations during different types of volcanic activity in order to assess the utility of OMI for volcano monitoring. We estimate plume heights for the different styles of activity observed and assess whether this can explain the differences in the ability of OMI to detect SO_2 at this volcano. We provide evidence from the 2008–2010 degassing record that shows that OMI detects SO_2 more frequently during eruptive activity than during periods of quiescence and we explore the mechanisms that might cause this.

2. Soufrière Hills Volcano and observations of SO_2 emissions

Soufrière Hills Volcano, Monserrat is a dome-forming andesitic volcano located within the Lesser Antilles island arc in the Caribbean (16.7° N, 62.2° W). The current eruption began in 1995, undergoing periods of quiescence with passive degassing interspersed with 5 phases of active lava extrusion. During the periods of active extrusion, the volcano displayed cycles of dome-forming and large explosive collapses. The last period of active extrusion ended in a large dome collapse on 11 February 2010. Since that time, the volcano has continued to passively degas.

The SO_2 emissions from Soufrière Hills are monitored using a ground-based array of Ocean Optics UV spectrometers, with the data processed using Differential Optical Absorption Spectrometry (DOAS) (Edmonds et al., 2003a). The long-term SO_2 flux has been approximately constant (over months-years timescales) since the start of the eruption, during periods of both quiescence and during lava dome growth, with an average flux of 574 t/d (Christopher et al., 2010) to the end of

* Corresponding author at: AOPP, Dept. of Physics, University of Oxford, UK.
E-mail address: catherine.hayer@physics.ox.ac.uk (C.S. Hayer).

http://dx.doi.org/10.1016/j.jvolgeores.2016.01.014

Phase 5. Since the end of Phase 5, the average has been 375 t/d. However, the DOAS record does display a second-order variability with a multi-year periodicity (Christopher et al., 2014).

When the plume is located higher in the atmosphere, there are some challenges with the DOAS retrieval. This is because of the geometry of the retrieval and the longer pathlength from the instrument. Due to the viewing geometry of the ground-based spectrometer systems, it is impossible to determine if a plume is small with a lower altitude or is larger but higher in the atmosphere when using a single instrument (Edmonds et al., 2003a). When the plume is higher in the atmosphere, the photons travel a longer pathlength. This can lead to a light dilution effect, as photons are scattered away from the instrument (Kern et al., 2010) which in turn can lead to an underestimate of the SO_2 loading. The presence of ash in the plume, a common occurrence at a dome-forming volcano like Soufrière Hills, can also cause errors in retrievals (Edmonds et al., 2003a). The optical thickness of the ash reduces or completely blocks sunlight from penetrating the plume, artificially reducing the retrieved SO_2 mass or rendering the retrieval impossible. If a plume is emplaced at a high altitude, it may be influenced by a different weather pattern to that at lower altitudes. Since the locations of the DOAS instruments are fixed, if the plume does not overpass them, a retrieval is impossible. All of these effects are more important for high altitude plumes, and so are likely to be associated with explosive events.

Satellite instruments have been observing volcanic SO_2 emissions since the 1982 eruption of El Chichón when the plume was observed by the Total Ozone Mapping Spectrometer (TOMS) (Mayberry et al., 2002). Since then, a number of different instruments have been used to monitor volcanoes and observe volcanic eruptions. These have included UV and IR instruments, such as the Ozone Monitoring Instrument (OMI), the Global Ozone Monitoring Experiment (GOME), the Atmospheric InfraRed Sounder (AIRS) and the Infrared Atmospheric Sounding Instrument (IASI) (Carn and Prata, 2010; Theys et al., 2013). The low ambient concentrations of SO_2 make it ideal for monitoring purposes, compared to the more abundant volcanic gases of CO_2 and H_2O.

OMI is an instrument on board the polar orbiting NASA Aura platform, overpassing Montserrat twice daily, at 01:45 and 13:45 local time (05:45 and 17:45 UTC). Since OMI is a UV instrument, it is only able to make measurements on the day side of the orbit (13:45 LT; 17:45 UTC). The orbital geometry of the satellite means that it takes a single daily snapshot of the SO_2 atmospheric loading rather than making a continuous flux measurement. Data are not returned by OMI on some days, for example when the swath of the instrument does not cover Montserrat or all the pixels are below the noise threshold of 0.4 DU. OMI's Charge Coupled Device (CCD) has been affected by a degeneration known as the OMI Row Anomaly (ORA), meaning various pixels across the CCD cannot be used. The ORA is thought to have been caused by movement of Aura's protective shield into OMI's field of view, partially blocking it. The degeneration began in August 2008 and has fluctuated over time, with more pixels becoming affected, but also with the regeneration of a few affected pixels. The ORA has been stable since July 2011 (Flower and Carn, 2015). The reduced spatial coverage caused by the ORA reduced the probability of observing the plume by 2% in Phase 4 and 12% in Phase 5.

SO_2 plumes have been observed by satellite instruments from Soufrière Hills since 1997. TOMS and OMI observations together have measured 0.5 Mt. of SO_2 released largely during major explosive activity, a contribution which represents around 13% of the total documented sulphur dioxide emission during the eruption up to the end of 2011 (Carn and Prata, 2010; Edmonds et al., 2014).

To date, there have been five phases of extrusive activity at SHV since 1995 (1) (Wadge et al., 2014). Since the new generation of satellites were not in orbit for the first two phases, and some not for the third phase, only the last two phases are considered in this paper. The fourth phase (Phase 4) began on 29 July 2008 and ended on 3 January 2009. On 6 October 2009, the volcano entered its fifth phase (Phase 5) of extrusive activity, involving lava dome growth and collapse, pyroclastic flows and explosions, which concluded on 11 February 2010 with a collapse of ~50 million m^3 of lava dome material and an explosion with a large tephra and gas plume (Cole et al., 2010, 2014). During most of Phase 5, the Soufrière Hills DOAS array was inoperative and the OMI observations were the most frequent and sometimes the only method of measuring SO_2 emission.

3. OMI measurements, retrievals and uncertainties

The OMI dataset used was the SO_2 retrieval, OMSO2 (OMI Team, 2012), obtained from the NASA Mirador data store (http://mirador.gsfc.nasa.gov/). The accuracy of the SO_2 retrieval is highly dependent upon the correct assumption of the Centre of Mass Altitude (CMA) of

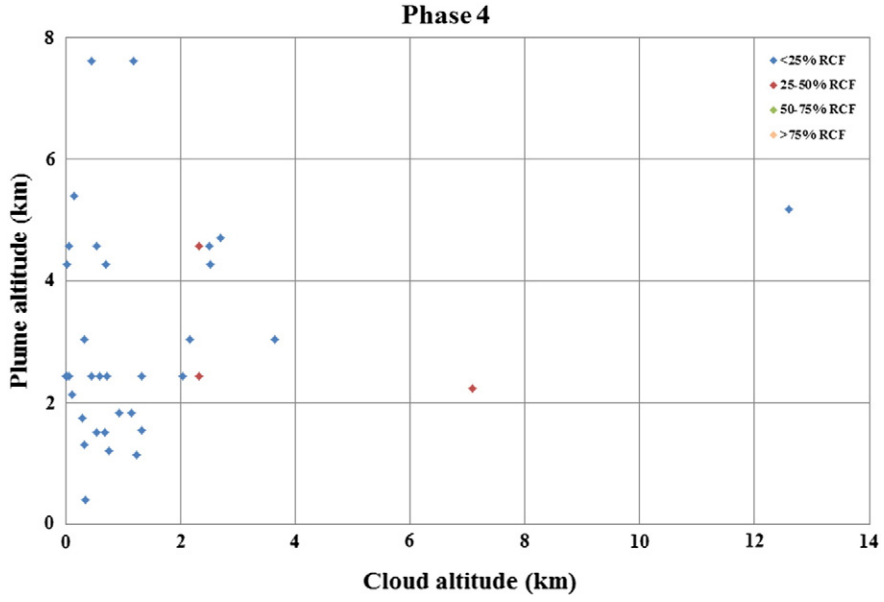

Fig. 1. Comparison of the altitude of the meteorological cloud (OMSO2 metadata) and the SO_2 plume (Washington VAAC VAA archive (Washington VAAC, 2016)) during Phase 4. The meteorological cloud altitude is an average over the region covered by the SO_2 plume. The colour of the diamonds indicates the percentage radiative cloud fraction, as denoted in the legend.

the SO_2 plume (Yang et al., 2007), but there are a number of other factors which also affect the retrieval, discussed below.

3.1. Radiative Cloud Fraction (RCF)

The fraction of the sky covered with meteorological cloud (reported as a fraction of 1) (RCF) is the biggest cause of error in the SO_2 retrieval, after those introduced by an incorrect CMA (Section 3.4). Thin, high altitude cirrus clouds are not expected to cause significant errors in the retrieval; however, thicker cloud can cause error (Yang et al., 2007). If the SO_2 plume is located below an optically thick layer of meteorological cloud, the cloud masks the SO_2 and this leads to an underestimate of the true SO_2 loading. If the SO_2 plume is located above a thick layer of cloud, this can artificially enhance the loading as more UV radiation is reflected off the cloud than would be off the ground (McCormick et al., 2013). Therefore the smaller the average RCF, the more reliable the retrieval. The plumes which are observed by OMI (SO_2 plume altitudes determined from Washington VAAC Volcanic Ash Advisory reports (Washington VAAC, 2016)) are generally higher than the surrounding meteorological cloud (meteorological cloud altitudes from metadata within the OMSO2 data set, generated using methods described by Joiner and Vasilkov (2006) and Joiner et al. (2010)); this was found to be true for 90% of days with a plume during Phase 4 and 84% of days during Phase 5 (Figs. 1 and 2). For these dates, the average RCF over the area covered by the plume is usually less than 0.25 (81% of dates for Phase 4 and 84% for Phase 5). The averaged RCF over a 2° area centred on Montserrat is also found to be less than 0.25 for 77% of days during Phase 4 and 93% of days during Phase 5. Analysis of the effect of the RCF on the CMA TRL and TRM (Section 3.4) retrievals indicates that when the RCF is below 0.2, the errors are dominated by noise from other sources (Carn et al., 2013). The errors are expected to increase linearly for RCFs greater than 0.2. The effect of cloud was also observed to be more pronounced on the TRL retrieval than on the TRM.

3.2. Sensor viewing angle

The sensor viewing angle (or zenith angle) varies across an instrument's swath. For OMI, the viewing angle reaches ±70° about the central viewing point (nadir). This change in the angle is caused by the curvature of the Earth and results in the pixels at the edge of the swath being significantly wider than those at the centre of the swath. At nadir, OMI's pixels are ~24 km wide; the outer pixels are ~155 km wide (Fig. 3). If a small plume is observed at the centre of the swath, it is likely to be covered by a number of pixels. However, at the outer edges, the plume may be smaller than one pixel, meaning the loading will be averaged over the whole pixel. If the SO_2 loading of the plume is very low, this could lead to the plume not being observed as the average loading value for the pixel may not exceed the detection threshold. The more oblique viewing angle at the edge of the swath will lead to a longer pathlength for the light passing through the plume, which will act to partially counteract the impact of this effect. There has, to date, been no extensive analysis of these 'edge effects'.

3.3. Solar zenith angle (SZA)

Since Aura is a sun-synchronous orbiter, the satellite equatorial overpass occurs at the same local time every day. Changes of the inclination of the Earth over the course of a year will cause only minor changes in the SZA at the Equator; however, since Montserrat is at 16 °N, there is slightly more variation in the SZA. Fig. 4a shows the variation of the SZA over Phase 4 and Fig. 4b shows the variation over Phase 5. Phase 4 occurred over a longer period and hence the variation is greater. The change in the SZA from one day to the next is small however. The seasonal variation of the SO_2 detection limit is primarily dependent on this change in SZA. As discussed by Carn et al. (2013, Fig. 12) and McCormick et al. (2013, Fig. 5), for mid (7.5 km) and lower (2.5 km)

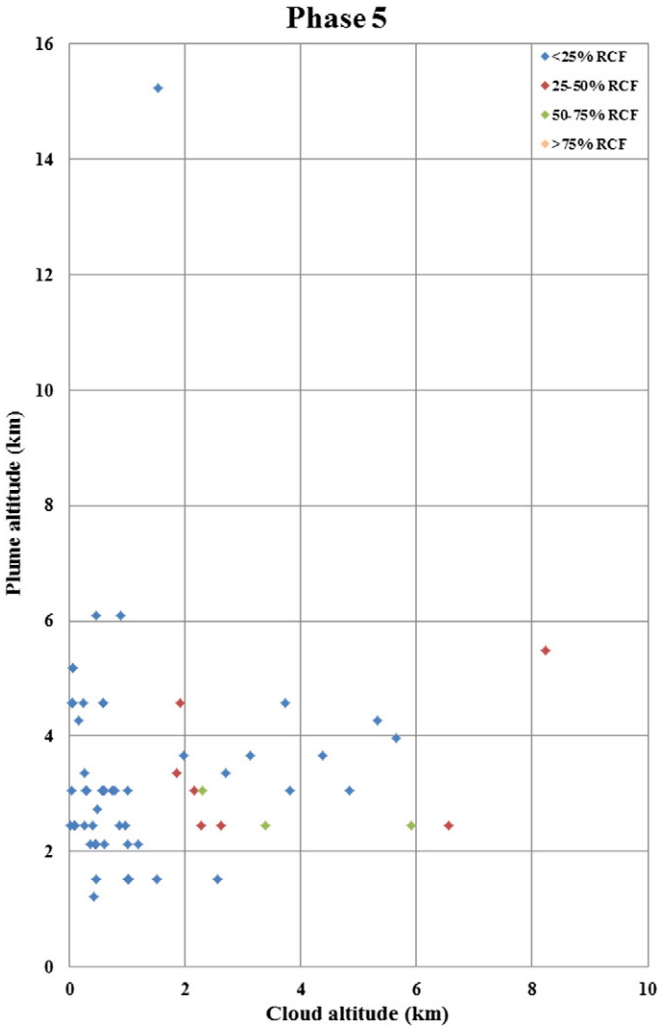

Fig. 2. Comparison of the altitude of the meteorological cloud (OMSO2 metadata) and the SO_2 plume (Washington VAAC VAA archive (Washington VAAC, 2016)) altitude during Phase 5. The colour of the diamonds indicates the percentage radiative cloud fractions, as denoted in the legend.

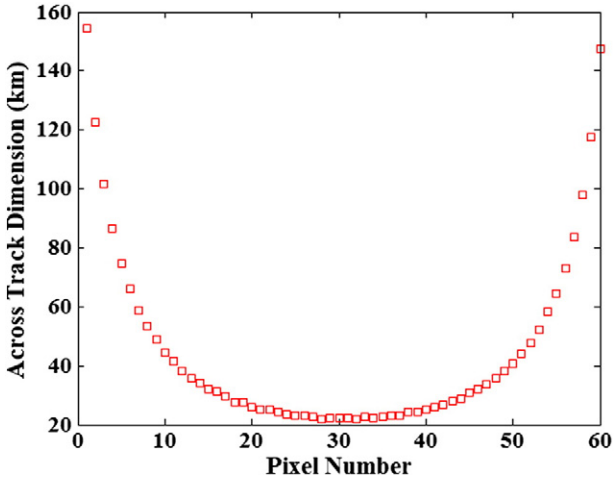

Fig. 3. Variation of the across-track width of OMI pixels with scan position (from OMI team, 2012, Fig. 7). As you move away from the centre of the swath, the curvature of the Earth causes the across-track dimension of the pixel to increase from ~24 km at the nadir point (centre) to ~155 km at the swath edge.

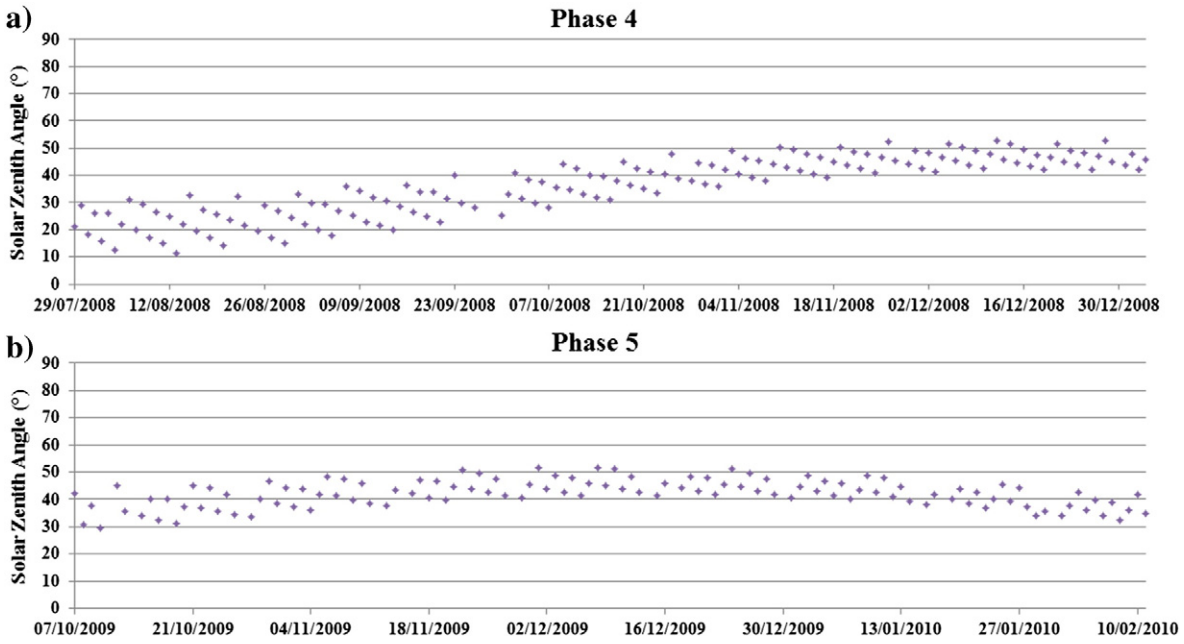

Fig. 4. Variation of the solar zenith angle over Phase 4 (a) and Phase 5 (b).

tropospheric plumes, the variation over the course of the year is small, of the order of 0.01 kt and <0.1 kt respectively. The impacts of each of these effects on the retrieval are small relative to the errors that may be introduced as a result of an incorrect assumption of the CMA (which can exceed 100%). They are therefore not considered further within this paper.

3.4. Centre of mass altitude

The SO_2 mass loading retrieval was initially performed for four assumed altitudes of the centre of mass of gas within the following four atmospheric layers: Planetary Boundary Layer (PBL), 0.9 km above the ground surface; Lower Troposphere (TRL), 2.5 km; Middle Troposphere (TRM), 7.5 km; and Lower Stratosphere (STL), 17.5 km. The mass loading was then interpolated linearly (Yang et al., 2007) between two of these CMA classes to the estimated altitude for the gas plume, usually obtained either from a Volcanic Ash Advisory (VAA) by the Washington Volcanic Ash Advisory Center (W-VAAC, Washington VAAC, 2016), estimated as the top of the ash cloud from satellite imagery, radiosonde soundings, pilot reports, or from observations made by the Montserrat Volcano Observatory (MVO) (Fig. 5). The VAA reports include the ash cloud top height and the centre of mass altitude of the SO_2 plume, which is required for the retrieval. However, ash plumes are regularly found slightly lower in the atmosphere than the corresponding SO_2 plume, thus reducing the mismatch (Mayberry et al., 2002). As the plume ages and sinks within the atmosphere, it becomes more likely that using the ash cloud top height will lead to an underestimate of the altitude of the CMA, which in turn will lead to an overestimate of the SO_2 loading in the plume (Yang et al., 2007).

During the retrieval, the altitude used for the CMA was derived from the VAA reports (Washington VAAC, 2016) where possible. For dates when these were not issued, a DOAS-derived altitude was used, if available, or the plume was assumed to be at the level of the TRL class (2.5 km).

Each CMA is associated with an a priori assumption on the shape and vertical distribution of SO_2 within the atmosphere. The use of an incorrect SO_2 profile, and hence CMA, was shown by Carn et al. (2013) to cause a significant overestimate of the atmospheric SO_2 loading if the plume was located above the assumed altitude and an underestimate if it was located below the assumed height. If the 2.5 km CMA is used and the plume is actually located higher than 2.5 km, the retrieval can produce an overestimate of the true atmospheric loading of SO_2, up to 175%. However, the impact of the plume being located lower on this kernel is less severe. For both the TRL (7.5 km) and STL (17 km) bands, the reverse is true. The impact of the plume being located higher than the assumed altitude is less severe, while the impact of the plume being located under the assumed altitude is greater, with up to a 60% underestimate of the atmospheric loading. The impact of meteorological cloud below the plume on the retrieval is limited if the plume is located at the assumed altitude or higher. However, if the plume is actually located lower than the assumed altitude, this leads to an overestimate in the atmospheric loading down to almost the level of the meteorological cloud. Below this, the retrieved loading drops off very quickly, due to the masking of the SO_2 plume beneath the meteorological cloud (Yang et al., 2007).

4. Results

The DOAS record shows that the SO_2 emission rate was variable during Phase 4, ranging from <100 to >2000 t/day (Fig. 6). There is no correlation between DOAS SO_2 emission rate and the explosive volcanic events, though this could be impacted by the timing of the event (UV spectroscopy is not possible during the night) or due to the ash content of the plume increasing the opacity of the plume (Fig. 6). During the 10–11 April 2011 eruption of Mt. Etna, ground-based DOAS underestimated the SO_2 loading of ash rich plumes by up to an order of magnitude (Boichu et al., 2015). OMI detected SO_2 infrequently between 29 July 2008 and 2 December 2008 (on average once every 4.6 days), and then more frequently from 3 December 2008 until 3 January 2009 (every 1.3 days). During the period 3 December 2008 to 3 January 2009 (Phase 4b), the lava dome grew at a rate of ~13 m^3s^{-1} (Wadge et al., 2014), and enhanced rockfall activity reflected this high rate of lava extrusion (Fig. 6), a behaviour previously seen during the eruption, as reported by Calder et al. (2005). During this period of lava extrusion, SO_2 emission rates measured by DOAS were mostly <1000 t/d and on average, lower than those for 29 July 2008 to 3 January 2009 (Fig. 6), during which time the lava extrusion rate was <1 m^3s^{-1} (Wadge et al., 2014).

During Phase 5, lava was extruded at an average rate of ~7 m^3s^{-1} (Stinton et al., 2014), accompanied by rockfalls, larger collapses

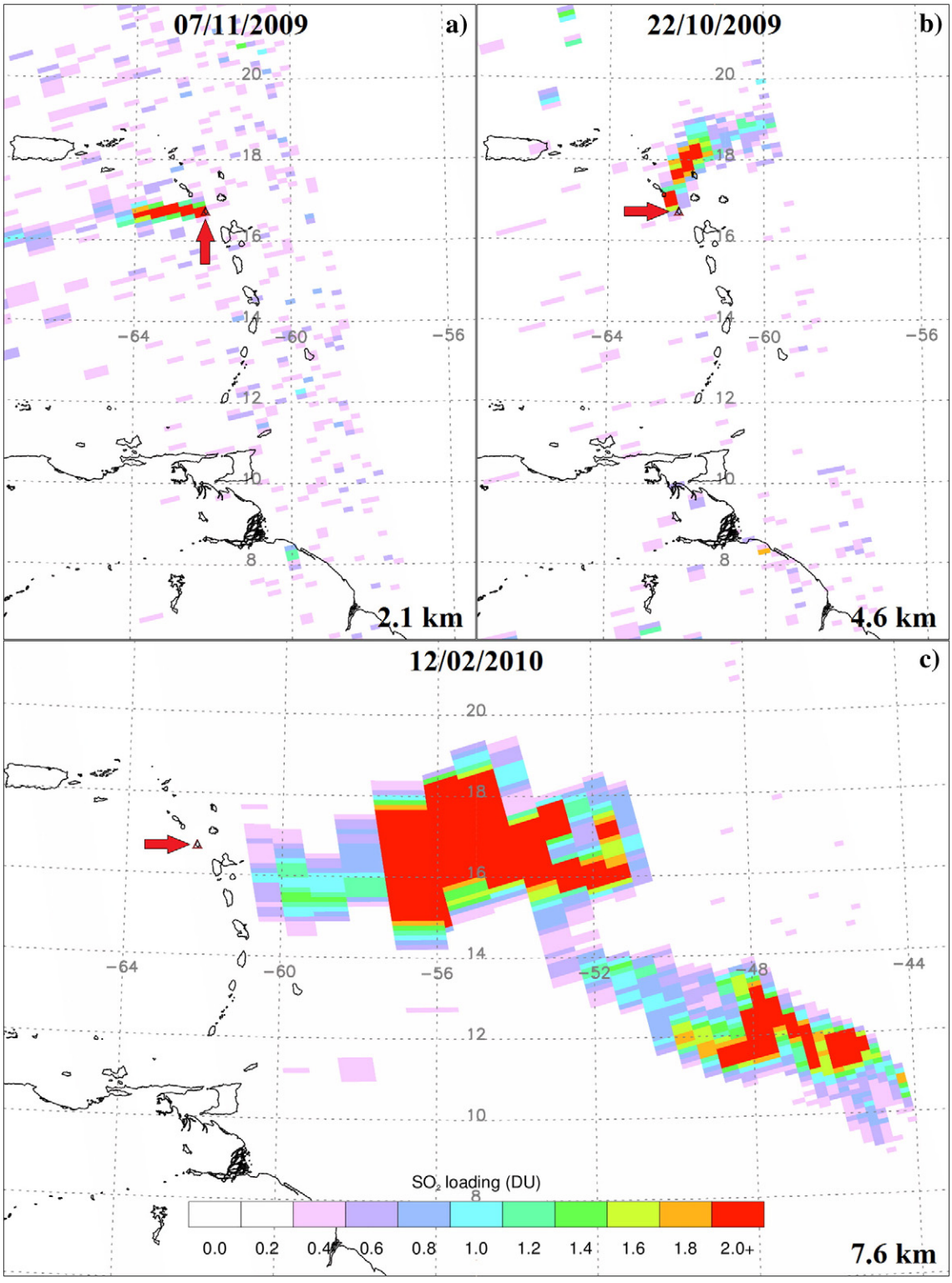

Fig. 5. Examples of SO_2 plumes, emitted from SHV (arrowed), as observed by OMI: (a) small (665 t); (b) medium (2147 t); (c) large (138,381 t). The altitude of each plume is shown. Note that the direction of the plume is controlled by local weather patterns, with the NE Trade Winds being dominant at lower tropospheric altitudes (a). Dates (dd/mm/yyyy) of the images and the latitude and longitude of the Eastern Caribbean are shown.

producing pyroclastic flows, and occasional Vulcanian explosions (Fig. 7; Komorowski et al., 2010). The activity level underwent strong cycles during this phase.

There is a general correlation between the OMI data and the rockfall seismicity data (Fig. 7b), particularly for October 2009. Specific daily correlations can also be seen: for example, high seismicity and SO_2 loading, together with large pyroclastic flows, occurred on 11th December 2009 (Fig. 7), but not in all cases. A large SO_2 signal persisted for 12 days as a result of the large dome collapse and Vulcanian explosion at the end of Phase 5, on 11th February 2010 (Figs. 5c; 7c). Conversely, at 14.49 local time on 8th January 2010, there was a large Vulcanian explosion, producing an 8 km eruption column, which did not produce a

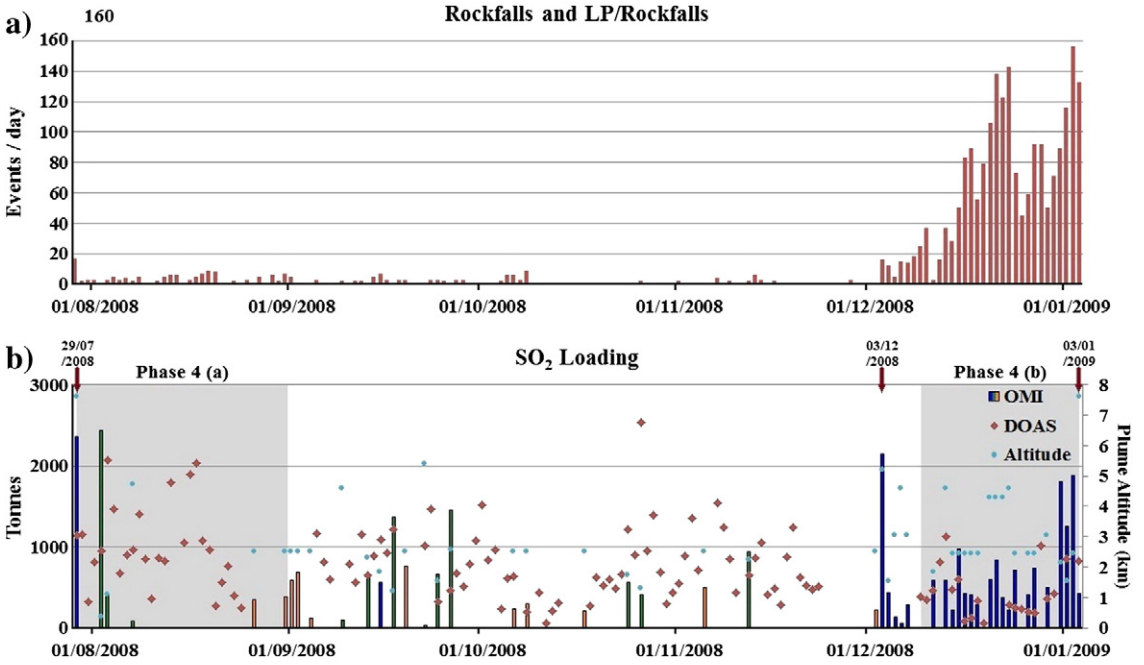

Fig. 6. Monitoring data for Phase 4: a) Rockfall seismicity; b) SO_2 records from DOAS and OMI along with the plume altitude. The data source for the altitude of the plume is denoted by the colour of the bars: blue = VAA; green = DOAS; orange = assumed altitude of 2.5 km. Red arrows show the 3 main Vulcanian explosions; shaded areas denote lava extrusion.

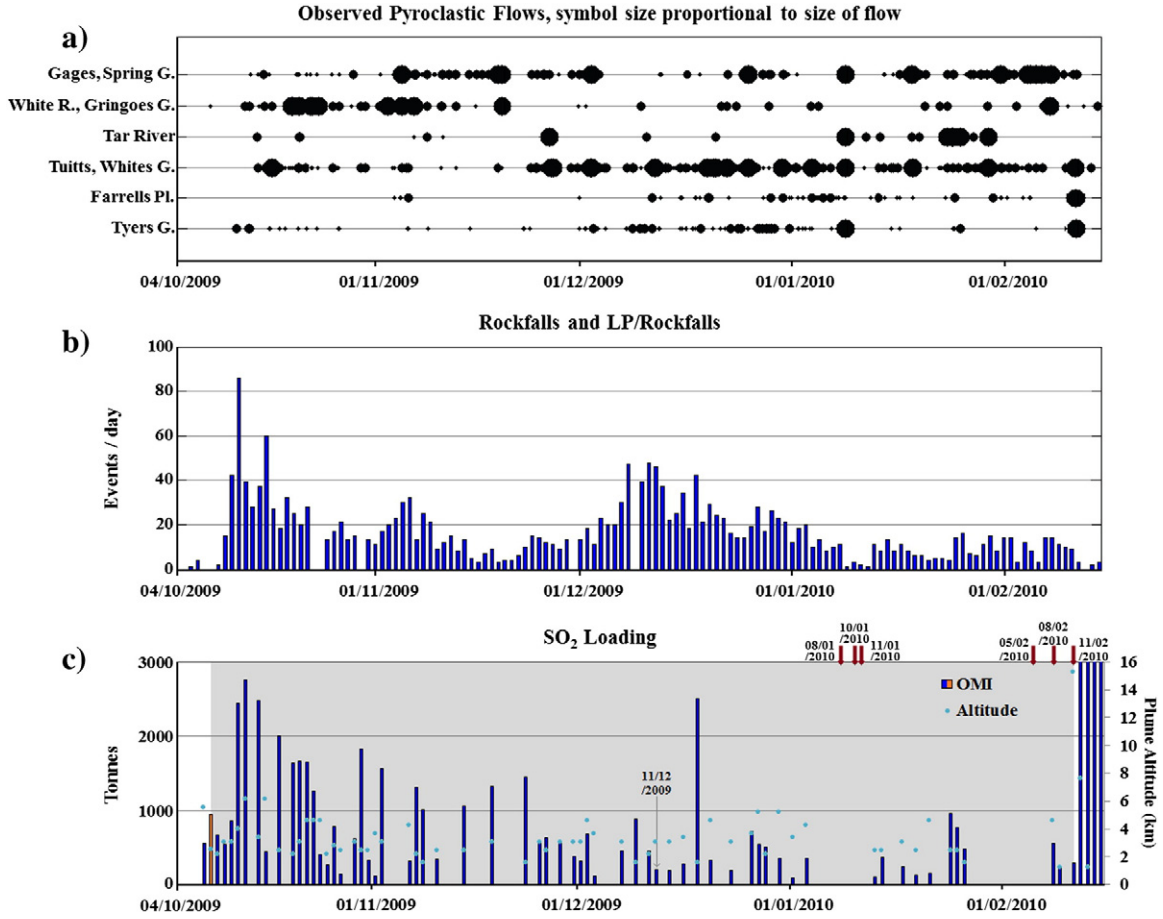

Fig. 7. Monitoring data for Phase 5: a) Pyroclastic flow location (y-axis) and size (circle diameter); b) Rockfall seismicity; c) SO_2 daily loading as measured by OMI and plume altitude. Coloured bars, red arrows and shaded areas as in Fig. 6 (a and b after Cole et al., 2010).

Table 1
Frequency of SO_2 signals observed by OMI before, during and after Phases 4 and 5.

Period	Dates	No. of days	Days with data available	Days with signals	% signals
Before Phase 4	21/02/2008–28/07/2008	159	153	20	13
Phase 4	29/07/2008–03/01/2009	159	147	49	33
After Phase 4	04/01/2009–11/06/2008	159	130	7	5
Before Phase 4b	27/06/2008–28/07/2008	32	31	7	23
Phase 4b	03/12/2008–03/01/2009	32	31	24	77
After Phase 4b	04/01/2009–04/02/2009	32	28	1	4
Before Phase 5	30/05/2009–05/10/2009	129	97	8	8
Phase 5	06/10/2009–11/02/2010	129	110	63	57
After Phase 5	24/02/2010–02/07/2010	129	96	18	19

signal detectable by OMI. This lack of signal may have been caused by two factors. First, the OMI overpass occurred 23 h after this explosion, such that a significant fraction of the SO_2 could have been removed from the atmosphere through chemical processing (Rodriguez et al., 2008), or made less detectable as the plume lost altitude. Second, the 8th January 2010 explosion is thought to have involved older, degassed dome material (Cole et al., 2010) and so perhaps there was only minimal contribution from the reservoirs of gas contained within the conduit or the magma chamber, both of which have been hypothesised as important sources of SO_2 in previous lava dome collapses (Edmonds et al., 2003b).

During Phase 5, OMI data were acquired over Montserrat on 110 of 129 days (Table 1), with a plume detected by OMI on 63 days (57%), but only on 13% of days from the non-extrusive periods before and after Phase 5. Over the whole of Phase 4, data were collected on 147 of 159 days, and a signal was observed on 49 days (33%). However, this includes the period of hiatus (October – November) when there was no lava extrusion. If we only consider the final part of the phase (03/12/08–03/01/09), then a signal was observed on 77% of days. For the quiescent periods before and after Phase 4, a signal was measured on 9% of days. For Phases 4 and 5 OMI detected 4–6 times as many signals during the periods of lava extrusion as during non-extrusion.

5. Discussion

We now evaluate the significance of the ability of OMI to detect SO_2 clouds preferentially during lava extrusion. We propose two causes: (1) an increase in the emission rate of SO_2 from the volcano or; (2) the increased lofting of gas to high altitudes. The first mechanism delivers more SO_2 into the atmosphere; the second results in OMI being able to observe the same amount of SO_2 at higher apparent loadings due to the plume being emplaced at higher altitudes. Higher altitude plumes mean a shorter path length with more backscattered photons crossing the plume, especially if the plume is located above the meteorological cloud, yielding a higher signal to noise ratio. SO_2 may also be removed more slowly at higher altitudes. An SO_2 removal rate of 30%/day has been proposed for Soufrière Hills, due to wet and dry deposition and conversion to sulphate (Rodriguez et al., 2008). Chemical processing in the plume is expected to be more rapid at lower altitudes due to clouds and rain (the former providing surfaces for heterogeneous chemistry and the latter removing sulphate aerosol from the atmosphere). Fig. 8 shows the distributions of observed plume altitudes. The mean altitude for Phase 4 was ~2.5 km and ~3 km for Phase 5.

During extrusive periods, the volatile transport from depth may increase for short periods, leading to an increase in SO_2 emission rate and more frequent detection by OMI. There are three possible mechanisms to achieve this: (1) a greater rate of supply of sulphur from the deep plumbing system; (2) an increase in the andesite lava extrusion rate, increasing the amount of SO_2 advected as a vapour phase; and (3) an increase in the permeability of the conduit to SO_2 rise. The presence of a lava dome at the top of the conduit, as was the case for both Phases 4 and 5, will tend to increase lithostatic pressure and lower permeability within the system (Woods et al., 2002). A larger dome may

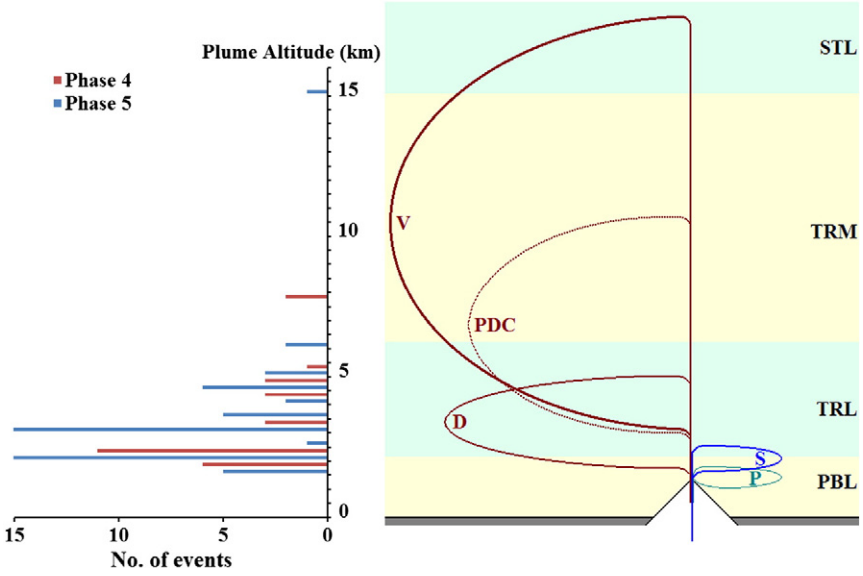

Fig. 8. Expected and observed plume altitudes at SHV. Left: Frequency of VAA plume heights for Phase 4 (red) and Phase 5 (blue). Right: OMI CMA atmospheric layers and the schematic SO_2 emplacement altitude ranges (curves) expected for each of the physical mechanisms envisaged at SHV (with an assumed vent altitude of 1 km a.s.l.). P = passive degassing; S = increased deep degassing or increased conduit permeability; V = Vulcanian explosion; PDC = co-pyroclastic flow plumes; D = hot dome.

also act as a high-level reservoir of SO_2 (Taisne and Jaupart, 2008). The higher overpressure from a larger dome may also increase the amount of gas that can be stored immediately below the dome. In Phase 5, there was a large explosion as the gas-rich core of the dome was partially exposed during the dome collapse on 11 February 2010, and which may have evacuated the magma within the conduit. The permeability of the whole system is at its highest after such events, leading to pulses of degassing (Edmonds et al., 2003a). However, the long-term DOAS-measured SO_2 degassing record does not show any significant difference in the rate of SO_2 degassing between extrusive and non-extrusive periods (Christopher et al., 2010), suggesting that variable SO_2 emission is not responsible for the OMI results. It is possible that the DOAS time series misses some of the higher altitude plumes, which are likely to have a higher SO_2 loading.

During extrusive periods, the plume attained higher mean altitudes than during non-extrusive periods. We consider three possible processes by which such lofting was achieved: (a) Vulcanian explosions; (b) buoyant plumes rising off pyroclastic flows following dome collapse ("co-pyroclastic flow clouds"); and (c) the higher temperature and buoyancy of the atmosphere above the hot dome during lava extrusion.

5.1. Vulcanian explosions

Vulcanian explosions inject gas and tephra plumes into the atmosphere with high initial momentum, and there are accurate observations of their altitude. Druitt et al. (2002) performed an extensive survey of the 88 Vulcanian explosions between August and October 1997. These events were associated with plume heights of 3–15 km (with a mean of ~9 km) measured using NOAA satellite data (heights around 20% lower were found using GOES satellite data), an average dense rock equivalent (DRE) volume of 3.8×10^5 m^3 and a range of $0.01–17.5 \times 10^5$ m^3. The explosions observed during Phases 4 and 5 reached a similar altitude range to the 1997 sequence of explosions (5–15 km) (Komorowski et al., 2010; Cole et al., 2014) albeit with a slightly smaller range in DRE volumes ($2–26 \times 10^5$ m^3).

Of the nine Vulcanian explosions in Phases 4 and 5 (Table 2), only four produced a large OMI signal, one produced a small signal and the remaining four did not produce a detectable plume. The three that produced the largest OMI observed signals (29 Jul. 2008, 3 Jan. 2009 and 11 Feb. 2010) erupted the largest proportions of pumiceous tephra, interpreted as the evacuation of magma from the conduit (Cole et al., 2014). The lack of a detected plume and minor pumice production for the other explosions suggests they were driven by shallow pressurization of the dome itself (e.g. Gottsmann et al. (2011)). A large SO_2 signal was produced on 3 December 2008, but there was very little pumice associated with this event. This explosion had the greatest seismic energy of all nine events, and a large amplitude strain signal. Gottsmann et al. (2011) interpreted this event as the result of rapid pressurization of the whole volcanic system with a concentration of gas beneath the lava dome driving the ballistic-dominated explosion.

The factors that mitigate against effective ground-based measurement of the SO_2 loading produced by Vulcanian explosions are the vertical nature of the plume, the high altitude of the plume and the ash content. For OMI, it is largely the timing of the overpass. If the explosion occurs just after overpass, then much of the SO_2 can be lost from the plume due to chemical processing and wet and dry deposition, before the next observation opportunity. The altitude of the SO_2-bearing plume may also decrease in the manner of ash-bearing plumes (Table 2), as observed in other eruptions (Dacre et al., 2011). This in turn will tend to reduce the strength of the signal.

Table 2
Vulcanian explosions from 2008 to 2010. ([1]Cole et al. (2014); [2] Washington VAAC VAA data (Washington VAAC, 2016)).

Date	Time (UTC)[1]	Hours to OMI overpass	Maximum plume height (km)[2]	Height at overpass (km)[2]	OMI loading (tonnes)
29/07/2008	03:30	14	12	8	2359
03/12/2008	01:34	16	12	5	2146
03/01/2009	11:04	7	11	8	419
08/01/2010	19:49	22	8	2	–
10/01/2010	05:28	12	7	2	–
11/01/2010	00:27	17	6	2	–
05/02/2010	17:49	24	7	2	–
08/02/2010	23:57	18	5	1	242 (09/02/10)
11/02/2010	16:49	1	15	15	291 (45,000: 12/02/10)

5.2. Co-pyroclastic flow plumes

The altitudes attained by buoyant plumes rising from pyroclastic flows are generally lower than those attained from Vulcanian explosions, as only thermal buoyancy forces are involved. We estimate plausible altitudes by assuming that the plume source can be treated as an 'instantaneous' event, which requires the rise time of the plume to be less than the release time (Woods and Kienle, 1994). This is reasonable if the elutriation time of the hot tephra and gas out of the flow and into the plume is less than the plume rise time. There are very limited data on pyroclastic flow plume rise times, however the average rise time of pyroclastic flow plumes during the 1990 Redoubt eruption was 200–500 s (Woods and Kienle, 1994) and during the Mt. St. Helens 1981 eruption, 350–500 s (Woods and Wohletz, 1991) and we assume these rise times are typical. The emplacement time for individual pyroclastic flows at Soufrière Hills is typically 120–180 s, validating the assumption that the source is 'instantaneous'.

Larger collapse-derived pyroclastic flow plumes can attain heights of up to 10 km (e.g. 25th June 1997, Loughlin et al. (2002)) but there are few accurate observations. These flows typically have DRE volumes of $0.1–10 \times 10^6$ m^3; a lava density of 2400 kg m^{-3}; and a specific heat of 1100 J kg^{-1} K^{-1}. The temperature of typical flow deposits (as measured by Cole et al. (2002)) are up to ~900 K. Using an elutriation temperature of ~600 K, as suggested by Woods and Kienle (1994), produces a temperature change of ~300 K. The proportion of solids elutriated are in the range 4–16% (Bonadonna et al., 2002), and we assume that 10% of the total mass releases its heat content to the plume. The maximum plume height, H (m), of an instantaneous source with Q (Joules) available thermal energy, calculated from the above values, is given by:

$$H = 1.87 \times Q^{1}/_{4}$$

and yields maximum plume heights of 3.2, 5.7 and 10.1 km for flow volumes of 0.1, 1.0 and 10×10^6 m^3 respectively (Morton et al., 1956).

5.3. Hot dome plumes

During periods of enhanced lava extrusion rate, hot lava extruded at the surface of the dome leads to an increase in the average surface temperature of the dome. Gas leaving the dome entrains the surrounding air that has been heated by the dome surface, making it more buoyant and increasing the altitude at which the gas-rich plume attains its level of neutral buoyancy.

The average volumetric lava flux in Phase 5 was about 6 m^{3}s^{-1}. Wooster et al. (1997) calculated that the thermal power emitted by the 1991–1993 lava flow on Mount Etna was 1–10 GW from a similar lava flux. The proportion of the total power emitted via convection ranged from 30 to 50%. The mechanism of convective heat transfer from a defined source area is also employed to study forest fires. Harrison and Hardy (2002) found an empirical relationship between

the maximum observed plume height, H (m) and the maximum power of the fire, P (GW):

$$H \approx 1403 \times P^{0.36}.$$

For a fire with P in the range 1–10 GW, which is the range of convective power emission expected for Soufrière Hills, H ~ 1.4–3.2 km. This estimate does not include the effect of wind on the plume height, which generally results in a lower H for a given size of fire. Freitas et al. (2010) used a numerical model (3-D Active Tracer High resolution Atmospheric Model (ATHAM)) to investigate the effect of wind on the plume from a 0.1 km^2 fire. This is a similar surface area to that covered by the central core of the lava dome during Phase 5, which is estimated as 0.07 km^2 (the area covered by the core and talus combined is estimated as 0.8 km^2). The heat flux from this size of fire was estimated at 80 kWm^{-2}, which produces a total energy emission of 8 GW—the same order of magnitude as that expected from SHV. The maximum plume height for the 0.1 km^2 fire was 3.3 km in calm conditions and 1.7 km for the windy case, when the plume was bent over. We would therefore expect a plume within the range 1.5–4 km during active lava extrusion.

The estimated ranges in altitude of the SO_2 plumes for the separate mechanisms described are shown in Fig. 8: Vulcanian explosions (3–15 km), co-pyroclastic flows (3–10 km), hot lava domes (1.5–4 km), and enhanced supply of SO_2 from depth (1.5–2 km). Most of the OMI signals recorded during Phases 4 and 5 were in the PBL and the lower troposphere (1.5–6 km) (Fig. 8). Those signals in the PBL are likely to have been formed by an enhanced rate of SO_2 degassing or by lofting above a hot lava dome. The plumes in the lower troposphere are likely to have been formed by lofting due to co-pyroclastic flows or above hot domes.

Some of the VAA values of Fig. 8 are probably underestimates. For tephra-rich plumes, two distinct components tend to separate within 24 h of emplacement, with a lighter SO_2-rich plume at a greater altitude than that of the tephra plume (Mayberry et al., 2002).

6. Conclusions

In conclusion, our study of the 2008–2010 SO_2 release from Soufrière Hills shows that:

i) During "passive" degassing, when no lava is being extruded, SO_2 loads in the atmosphere are up to six times less likely to be measured by OMI than during periods of lava extrusion.
ii) This variability in OMI detection capability is probably usually caused, not by real changes in the gas flux from the volcano, but by lofting of the gas plume during vigorous dome growth to 1.5 to 6 km above the volcano.
iii) Lofting of SO_2 is produced in three main ways: by Vulcanian explosions (3–15 km), by co-pyroclastic flow plumes (3–10 km) and by buoyant rise above the hot surface of the lava dome (1.5–4 km).
iv) Some Vulcanian explosions, involving magma from the conduit, show strong SO_2 signals, others just involving explosions within the dome, do not. This corroborates the mechanisms proposed by Komorowski et al. (2010); Gottsmann et al. (2011) and Cole et al. (2010).
v) OMI measurements will detect SO_2 loading events, due to Vulcanian explosions for example, that will be missed or underestimated by ground-based measurement systems, due to the increased path length caused by the altitude and the ash loading of the plume (Boichu et al., 2015).

OMI, and other satellite-based instruments, are biased towards measurements of emissions from eruptive volcanoes and so emissions into the troposphere by persistently degassing volcanoes, which make up the majority of SO_2 emissions, may be missed. Ground-based instruments are more likely to capture these emissions, but will miss plumes emplaced higher in the atmosphere. Since neither satellite- nor ground-based instruments favour retrieval of plumes emplaced in the middle atmosphere, it is expected that these plumes will be under-reported by an observation system involving both instrument types.

Acknowledgments

This work was supported by the NERC National Centre for Earth Observation (Theme 6: Dynamic Earth) grant, NE/E015093/1. The authors wish to thank R. Campion for his constructive review.

References

Boichu, M., Clarisse, L., Péré, J.-C., Herbin, H., Goloub, P., Thieuleux, F., Ducos, F., Clerbaux, C., Tanré, D., 2015. Temporal variations of flux and altitude of sulfur dioxide emissions during volcanic eruptions: implications for long-range dispersal of volcanic clouds. Atmos. Chem. Phys. 15, 8381–8400. http://dx.doi.org/10.5194/acp-15-8381-2015.

Bonadonna, C., Mayberry, G., Calder, E., 2002. Tephra fallout in the eruption of Soufrière Hills Volcano, Montserrat. In: Druitt, T.H., Kokelaar, B.P. (Eds.), The Eruption of Soufrière Hills Volcano, Montserrat, from 1995 to 1999. Geol. Soc., Lond., Mem 21, pp. 483–516. http://dx.doi.org/10.1144/GSL.MEM.2002.021.01.22.

Calder, E., Cortes, J., Palma, J., Luckett, R., 2005. Probabilistic analysis of rockfall frequencies during an andesite lava dome eruption: the Soufrière Hills Volcano, Montserrat. Geophys. Res. Lett. 32, L16309. http://dx.doi.org/10.1029/2005GL023594.

Carn, S., Prata, F., 2010. Satellite-based constraints on explosive SO_2 release from Soufrière Hills Volcano, Montserrat. Geophys. Res. Lett. 37, L00E22. http://dx.doi.org/10.1029/2010GL044971.

Carn, S.A., Krotkov, N.A., Yang, K., Krueger, A.J., 2013. Measuring global volcanic degassing with the Ozone Monitoring Instrument (OMI). In: Pyle, D.M., Mather, T.A., Biggs, J. (Eds.), Remote Sensing of Volcanoes and Volcanic Processes: Integrating Observations and Modelling. Geol. Soc., Lond., Spec. Publ. 380, pp. 229–257. http://dx.doi.org/10.1144/SP380.12.

Christopher, T., Edmonds, M., Humphreys, M., Herd, R., 2010. Volcanic gas emissions from Soufrière Hills Volcano, Montserrat 1995–2009, with implications for mafic magma supply and degassing. Geophys. Res. Lett. 37, L00E04. http://dx.doi.org/10.1029/2009GL041325.

Christopher, T., Edmonds, M., Taisne, B., Odbert, H., Costa, A., Hards, V., Wadge, G., Zellmer, G.F., 2014. Periodic sulphur dioxide degassing from the Soufrière Hills Volcano related to deep magma supply. In: Edmonds, M., Straub, S.M. (Eds.), The Role of Volatiles in the Genesis, Evolution and Eruption of Arc Magmas. Geol. Soc., Lond., Spec. Publ. 140, pp. 123–141. http://dx.doi.org/10.114/SP410.11.

Cole, P., Calder, E., Sparks, R.S.J., 2002. Deposits from dome-collapse and fountain-collapse pyroclastic flows at Soufrière Hills Volcano, Montserrat. In: Druitt, T.H., Kokelaar, B.P. (Eds.), The Eruption of Soufrière Hills Volcano, Montserrat, from 1995 to 1999. Geol. Soc., Lond., Mem. 21, pp. 231–262. http://dx.doi.org/10.1144/GSL.MEM.2002.021.01.11.

Cole, P., Bass, V., Christopher, T., 2010. Report to the 14th Scientific Advisory Committee on Montserrat Volcanic Activity. [Online]. Available at: www.mvo.ms.

Cole, P.D., Smith, P.J., Stinton, A.J., Odbert, H.M., Bernstein, M.L., Komorowski, J.C., Stewart, R., 2014. Vulcanian explosions at Soufrière Hills Volcano, Montserrat between 2008 and 2010. In: Wadge, G., Robertson, R., Voight, B. (Eds.), The Eruption of Soufrière Hills Volcano, Montserrat from 2000 to 2010. Geol. Soc., Lond., Mem. 39, pp. 93–111. http://dx.doi.org/10.1144/M39.5.

Dacre, H., Grant, A., Hogan, R., 2011. Evaluating the structure and magnitude of the ash plume during the initial phase of the 2010 Eyjafjallajökull eruption using lidar observations and NAME simulations. J. Geophys. Res. 116, D00U03. http://dx.doi.org/10.1029/2011JD015608.

Druitt, T., Young, S., Baptie, B., 2002. Episodes of cyclic Vulcanian explosive activity with fountain collapse at Soufrière Hills Volcano, Montserrat. In, Druitt, T.H. & Kokelaar, B.P. (eds.) The eruption of Soufrière Hills Volcano, Montserrat, from 1995 to 1999. Geol. Soc. Lond. Mem. 21, 281–306. http://dx.doi.org/10.1144/GSL.MEM.2002.021.01.13.

Edmonds, M., Herd, R., Galle, B., Oppenheimer, C., 2003a. Automated, high time-resolution measurements of SO_2 flux at Soufrière Hills Volcano, Montserrat. Bull. Volcanol. 65, 578–586. http://dx.doi.org/10.1007/s00445-003-0286-x.

Edmonds, M., Oppenheimer, C., Pyle, D., 2003b. SO_2 emissions from Soufrière Hills Volcano and their relationship to conduit permeability, hydrothermal interaction and degassing regime. J. Volcanol. Geotherm. Res. 124, 23–43. http://dx.doi.org/10.1016/S0377-0273(03)00041-6.

Edmonds, M., Humphreys, M.C.S., Hauri, E.H., Herd, R.A., Wadge, G., Rawson, H., Ledden, R., Plail, M., Barclay, J., Aiuppa, A., Christopher, T.E., Guidice, G., Guida, R., 2014. Pre-eruptive vapour and its role in controlling eruption style and longevity at Soufrière Hills Volcano. In: Wadge, G., Robertson, R., Voight, B. (Eds.), The eruption of Soufrière Hills Volcano, Montserrat from 2000 to 2010. Geol. Soc., Lond., Mem. 39, pp. 291–315. http://dx.doi.org/10.1144/M39.16.

Flower, V.J.B., Carn, S.A., 2015. Characterising volcanic cycles at Soufrière Hills Volcano, Montserrat: time series analysis of multi-parameter satellite data. J. Volcanol. Geotherm. Res. 304, 82–93. http://dx.doi.org/10.1016/j.jvolgeores.2015.07.035.

Freitas, S., Longo, K., Trentmann, J., Latham, D., 2010. Technical note: sensitivity of 1-D smoke plume rise models to the inclusion of environmental wind drag. Atmos. Chem. Phys. 10, 585–594. http://dx.doi.org/10.5194/acp-10-585-2010.

Gottsmann, J., Angelis, S.D., Fournier, N., 2011. On the geophysical fingerprint of Vulcanian explosions. Earth Planet. Sci. Lett. 306, 98–104. http://dx.doi.org/10.1016/j.epsl.2011.03.035.

Harrison, H., Hardy, C., 2002. Plume rise from GigaWatt fires: observations and models. [Online]. Available at: http://www.atmos.washington.edu/~harrison/reports/plume3.pdf.

Joiner, J., Vasilkov, A., 2006. First results from the OMI rotational raman scattering cloud pressure algorithm. IEEE Trans. Geosci. Remote Sens. 44, 1272–1282. http://dx.doi.org/10.1109/TGRS.2005.861385.

Joiner, J., Vasilkov, A., Bhartia, B., Wind, G., Platnick, S., Menzel, W., 2010. Detection of multi-layer and vertically-extended clouds using A-Train sensors. Atmo. Meas. Tech. 3, 233–247. http://dx.doi.org/10.5194/amt-3-233-2010.

Kern, C., Deutschmann, T., Vogel, L., Wohrbach, M., Wagner, T., Platt, U., 2010. Radiative transfer corrections for accurate spectroscopic measurements of volcanic gas emissions. Bull. Volcanol. 72, 233–247. http://dx.doi.org/10.1007/s00445-009-0313-7.

Komorowski, J.-C., Legendre, Y., Christopher, T., 2010. Insights into processes and deposits of hazardous Vulcanian explosions at Soufrière Hills Volcano during 2008 and 2009 (Montserrat, West Indies). Geophys. Res. Lett. 37, L00E19. http://dx.doi.org/10.1019/2010GL042558.

Loughlin, S., Calder, E., Clarke, A., 2002. Pyroclastic flows and surges generated by the 25 June 1997 dome collapse, Soufrière Hills Volcano, Montserrat. In: Druitt, T.H., Kokelaar, B.P. (Eds.), The Eruption of Soufrière Hills Volcano, Montserrat, from 1995 to 1999. Geol. Soc., Lond., Mem. 21, pp. 191–209. http://dx.doi.org/10.1144/GSL.MEM.2002.021.01.09.

Mayberry, G., Rose, W., Bluth, G., 2002. Dynamics of volcanic and meteorological clouds produced on 26 December (Boxing Day) 1997 at Soufrière Hills Volcano, Montserrat. In: Druitt, T.H., Kokelaar, B.P. (Eds.), The Eruption of Soufrière Hills Volcano, Montserrat, from 1995 to 1999. Geol. Soc., Lond., Mem. 21, pp. 539–556. http://dx.doi.org/10.1144/GSL.MEM.2002.021.01.24.

McCormick, B.T., Edmonds, M., Mather, T.A., Campion, R., Hayer, C.S.L., Thomas, H.E., Carn, S.A., 2013. Volcano monitoring applications of the Ozone Monitoring Instrument (OMI). In: Pyle, D.M., Mather, T.A., Biggs, J. (Eds.), Remote Sensing of Volcanoes and Volcanic Processes: Integrating Observations and Modelling. Geol. Soc., Lond., Spec. Publ. 380, pp. 259–291. http://dx.doi.org/10.1144/SP380.11.

Morton, B., Taylor, G., Turner, J., 1956. Turbulent gravitational convection from maintained and instantaneous sources. Proc. R. Soc. A234, 21–42. http://dx.doi.org/10.1098/rspa.1956.0011.

OMI Team, 2012. Ozone Monitoring Instrument (OMI) Data User's Guide. [Online]. Available at: http://disc.sci.gsfc.nasa.gov/Aura/additional/documentation/README.OMI_DUG.pdf.

Oppenheimer, C., Scaillet, B., Martin, R., 2011. Sulfur degassing from volcanoes: source conditions, surveillance, plume chemistry and earth system impacts. Rev. Mineral. Geochem. 73, 363–421. http://dx.doi.org/10.2138/rmg.2011.73.13.

Rodriguez, L., Watson, I., Edmonds, M., 2008. SO_2 loss rates in the plume emitted by Soufrière Hills Volcano, Montserrat. J. Volcanol. Geotherm. Res. 173, 135–147. http://dx.doi.org/10.1016/j.jvolgeores.2008.01.003.

Shinohara, H., 2008. Excess degassing from volcanoes and its role on eruptive and intrusive activity. Rev. Geophys. 46, RG4005. http://dx.doi.org/10.1029/2007RG000244.

Stinton, A.J., Cole, P.D., Odbert, H.M., Christopher, T., Avard, G., Bernstein, M., 2014. Dome growth and valley fill during Phase 5 (8 October 2009–11 February 2010) at the Soufrière Hills Volcano, Montserrat. In: Wadge, G., Robertson, R., Voight, B. (Eds.), The Eruption of Soufrière Hills Volcano, Montserrat from 2000 to 2010. Geol. Soc., Lond., Mem. 39, pp. 113–131. http://dx.doi.org/10.1144/M39.6.

Taisne, B., Jaupart, C., 2008. Magma degassing and intermittent lava dome growth. Geophys. Res. Lett. 35, L20310. http://dx.doi.org/10.1029/2008GL035432.

Theys, N., Campion, R., Clarisse, L., Brenot, H., van Gent, J., Dils, B., Corradini, S., Merucci, L., Coheur, P.-F., Van Roozendael, M., Hurtmans, D., Clerbaux, C., Tait, S., Ferrucci, F., 2013. Volcanic SO_2 fluxes derived from satellite data: a survey using OMI, GOME-2, IASI and MODIS. Atmos. Chem. Phys. 13, 5945–5968. http://dx.doi.org/10.5194/acp-13-5954-2013.

Wadge, G., Voight, B., Sparks, R.S.J., Cole, P.D., Loughlin, S.C., Robertson, R.E.A., 2014. An overview of the eruption of Soufrière Hills Volcano, Montserrat from 2000 to 2010. In: Wadge, G., Robertson, R., Voight, B. (Eds.), The Eruption of Soufrière Hills Volcano, Montserrat from 2000 to 2010. Geol. Soc., Lond., Mem. 39, pp. 1–39. http://dx.doi.org/10.1144/M39.1.

Washington VAAC, VAA report archive, accessed 2016, [Online]. Available at http://www.ssd.noaa.gov/VAAC/archive.html.

Woods, A., Kienle, J., 1994. The dynamics and thermodynamics of volcanic clouds: theory and observations from the April 15 and April 21 1990 eruptions of Redoubt Volcano, Alaska. J. Volcanol. Geotherm. Res. 62, 273–299. http://dx.doi.org/10.1016/0377-0273(94)90037-X.

Woods, A.W., Wohletz, K., 1991. Dimensions and dynamics of co-ignibrite eruption columns. Nature 350, 225–227. http://dx.doi.org/10.1038/350225a0.

Woods, A., Sparks, R., Richie, L., 2002. The explosive decompression of a pressurised volcanic dome: the 26 December 1997 collapse and explosion at Soufrière Hills Volcano, Montserrat. In: Druitt, T.H., Kokelaar, B.P. (Eds.), The Eruption of Soufrière Hills Volcano, Montserrat, from 1995 to 1999. Geol. Soc., Lond., Mem. 21, pp. 457–465 (doi.org/10. 1144/GSL.MEM.2002.021.01.20).

Wooster, M., Wright, R., Blake, S., Rothery, D., 1997. Cooling mechanisms and an approximate thermal budget for the 1991–1993 Mount Etna lava flow. Geophys. Res. Lett. 24, 3277–3280. http://dx.doi.org/10.1029/97GL03166.

Yang, K., Krotkov, N., Krueger, A., 2007. Retrieval of large volcanic SO_2 columns from the Aura Ozone Monitoring Instrument: comparison and limitiations. J. Geophys. Res. 112, 1–14. http://dx.doi.org/10.1029/2007JD008825.